Transactions on Aerospace Research eISSN 2545-2835, VOL. 272, NO. 3/2023, 16-27
DOI: 10.2478/tar-2023-0014

SOLID ROCKET BOOSTERS SEPARATION SYSTEM DEVELOPMENT FOR THE ILR-33 AMBER 2K ROCKET

Jan Kierski*, **Arthur Pazik**, **Dawid Cieśliński**
Space Technologies Center, Łukasiewicz Research Network – Institute of Aviation,
Al. Krakowska 110/114, 02-256 Warsaw, Poland

Abstract

The paper presents the development process of the solid rocket boosters (SRBs) separation system of the ILR-33 AMBER 2K rocket. A redesign of the system was required due to the development of new, larger SRBs. The main system requirements were transmission of forces and moments between the SRBs and the main stage, execution of the separation process at a given moment in flight and mechanical integration simplification. A set of aerodynamics calculations were performed. With the use of computational fluid dynamics software, forces acting on the booster during separation for several angles of attack, as well as the critical booster deflection angle, have been determined. Next, a mathematical model was created to define the load spectrum acting on the system during the flight and separation phases, covering both static and dynamic loads. All the internal and external force sources were considered. A series of motion dynamics simulations were conducted for representative flight cases. Then, the system operational parameters were verified with the use of dedicated ground test facilities. Necessary calibrations of the mathematical model were then implemented, leading to a high level of confidence with the empirical data obtained, thereby leading to a successful system qualification for the flight campaign.

Keywords: sounding rocket; solid rocket booster; ILR-33 AMBER 2K; modelling; flight dynamics; ground testing
Type of the work: research article

Abbreviations:

CAD, computer aided design;
CFD, computational fluid dynamics;
DOF, degrees of freedom;
IoA, Łukasiewicz Research Network – Institute of Aviation;
SRB, solid rocket booster.

1. INTRODUCTION

Suborbital rockets are being widely used since the beginning of space exploration as a cheap and effective way of carrying out atmosphere sounding, suborbital experiments and various scientific research activities, as well as technology maturing and validation platforms [1,2]. In terms of design, we can divide them into single stage and multistage constructions. Two main multistage designs have been developed: serial staging, with stages mounted one on top of another, and parallel staging, where stages are attached

* Corresponding Author: jan.kierski@ilot.lukasiewicz.gov.pl
ARTICLE HISTORY **Received** 2022-09-26 **Revised** 2023-05-19 **Accepted** 2023-05-29

alongside each other. The use of parallel staging in small suborbital rockets is not common, but has a number of advantages over serial staging, such as a significant length reduction and a greater acceleration, which leads to a reduction of wind sensibility at launch.

ILR-33 AMBER is a two-stage suborbital rocket, developed by Łukasiewicz Research Network, Institute of Aviation, and has been in deployment since 2014. Its propulsion system consists of a hybrid rocket motor that uses high-test peroxide (98%) as an oxidiser and two strap-on solid rocket boosters (SRBs) [3,4]. Since 2019, a new 2K version of the rocket is under development, with a series of modifications, including larger SRBs [5,6]. An improved SRBs separation system also had to be implemented, to fulfil design and safety requirements. The purpose of the separation system is to transmit loads between the main core and the SRBs and to safely discard the strap-on boosters after their burnout. A comparison of both versions is presented in Figure 1.

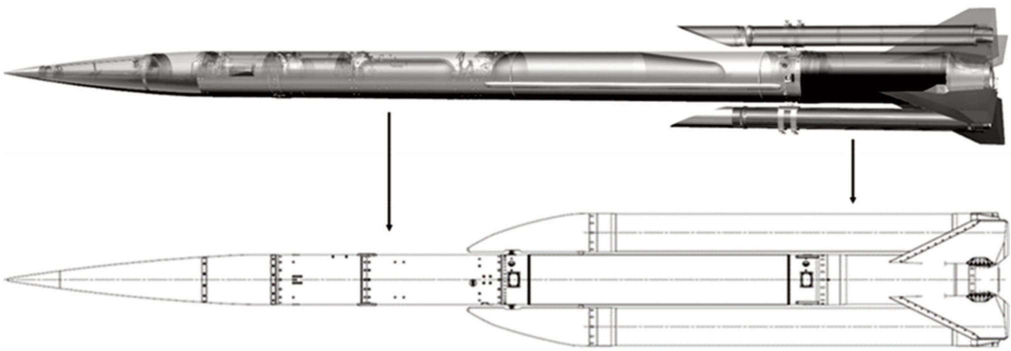

Figure 1. Comparison of both versions of the ILR-33 AMBER rocket:
top – original design; bottom – 2K version.

Design and simulation of separation of two bodies in relative motion in the atmosphere is a task of high complexity. Investigations on the aerodynamics of separation were conducted for several years, especially by Meakin [7] for the space shuttle. Dynamic models of separation for different designs were also analysed by Lochan et al. [8,9] and Seongjin et al. [10]. They conducted numerical analyses of separation dynamics with an integrated unsteady Navier–Stokes aerodynamics solver. Some commercially accessible solutions, such as STRLNCH from AMA [11], also allow the coupling between aerodynamics and separation dynamics, but these are dedicated mostly towards application in store separation from aircraft.

Although these investigations are a valuable source of information, they cannot be fully applicable to the case of the ILR-33 AMBER 2K rocket. Due to the aerodynamic shape, smaller size of the separated elements, quicker separation dynamics and requirements of separation on a vast range of dynamic pressures, a less conventional mechanical design had to be used, compared to the previous version of the rocket [3].

This meant that a dedicated approach to the problem was needed, in order to validate the system design and to qualify it for flight tests. It consisted of:

- a set of aerodynamics numerical analyses, based on computational fluid dynamics (CFD) and the wind tunnel investigation described and deepened herein;
- dynamics simulation analysis with a new, in-house developed 2D-3DOF software; and
- a series of ground tests of key components and of the whole system, designed to verify the mathematical models' correctness and components' functional requirements.

The aforementioned topics constitute the subject of this paper.

2. METHOD

2.1. Mechanical design

Each SRB separation system consists of three main subsystems, as shown in Figure 2: two attachment nodes and a repulsing system. The upper node is located in the nosecone of the boosters, right above the core stage's oxidiser tank (towards the main core nose). It is responsible for the release and carries side loads generated on the boosters. A pyro-mechanical release system is used in the upper node in order to release the fixation point. Its activation allows the repulsing system to push the boosters outwards.

In order to assure proper separation, a separate repulsing system was also introduced. It consists of a gas spring mounted in the nosecone of each booster, which, after the upper mount pyrotechnic release, pushes the SRB outwards. Once the gas spring is extended, exposing boosters on positive deflection angles, δ (measured as the angle between the booster's longitudinal axis and the main core longitudinal axis; a positive value of δ means that boosters' nosecones are deflected from the main core), the aerodynamic forces continue the ongoing outward motion. The margin for the δ angle sustainable for inducing positive aerodynamic moment for boosters' self-separation from the core is defined with reference to the angle of attack of the rocket in Figure 5.

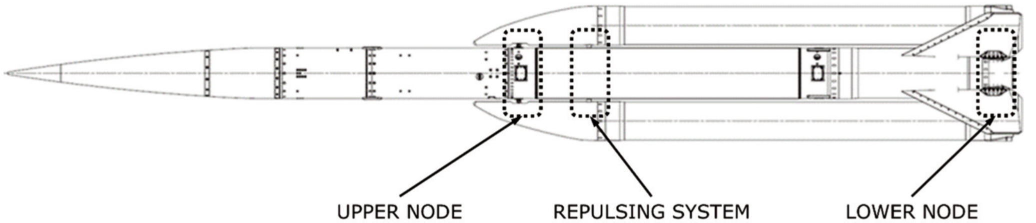

Figure 2. Components of the separation system.

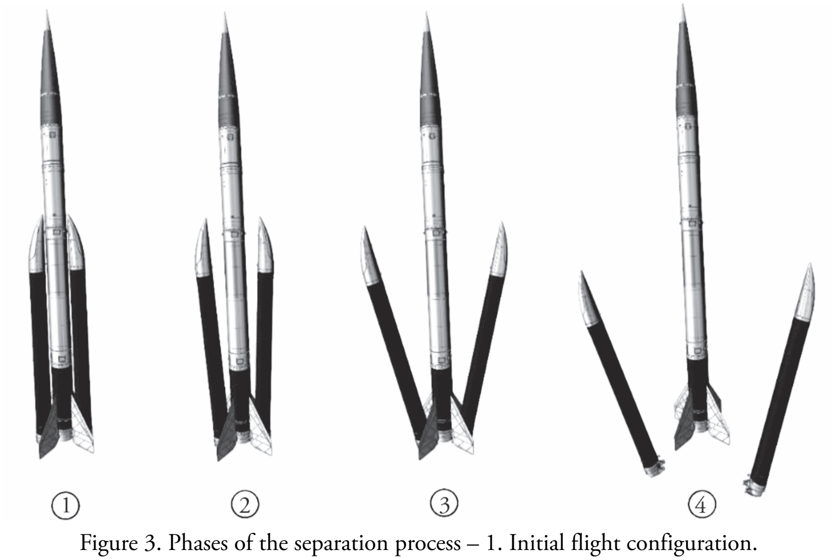

Figure 3. Phases of the separation process – 1. Initial flight configuration.
2. Upper node pyrotechnic release, the gas springs are pushing the boosters outwards. 3. Maximum deflection angle of the SRBs while being attached to the core, lower node release. 4. SRBs' separation and their ballistic flight (no recovery systems for SRB foreseen). SRB, solid rocket booster.

The lower node connects aft bodies of the main core and the SRBs and is a purely mechanical release system. It assures the separation at a specific angle between the boosters and the core. A ball joint system assures that all the longitudinal and side loads are transferred.

Boosters are kept attached by the lower nodes until the specific angle of their deflection is exceeded. The angle margin is foreseen in order to avoid the possibility of the SRBs' collision with the core of the rocket right after their separation, which is explained below. Above this angle, having an outward motion and due to the longitudinal aerodynamic forces, the boosters slip out and fall off, evading the rest of the rocket.

After burnout, the boosters are detached in the manner indicated in Figure 3. SRBs are expendable, which means that IoA does not attempt to recover them for reuse in subsequent flights.

2.2. Aerodynamics

CFD simulations were performed to determine aerodynamic characteristics of the rocket during the separation process for the following conditions:

- Mach numbers: from 0.4 to 2.3;
- Angles of attack for the whole rocket: α, –2°; 0° and 2° in the Y-Z plane. The convention of the α sign is presented in Figure 4;
- SRB deflection angles with respect to the main core: δ, 0°; 2°; 5°; 10° and 15°. The convention of the δ sign is presented in Figure 4.

The model was symmetric, and each numerical case considered that both the boosters are deflected by the same δ angle. Furthermore, as can be seen in Figure 4, simulating one α case, we obtain 'plus α' forces for the lower booster and 'minus α' forces for the upper booster. This assumption reduces the amount of the test cases required to be run. In the case of $\delta = 0°$, the CFD results have been correlated with wind tunnel tests [12], resultantly producing the following coefficients:

- Normal force coefficient (–) $c_Y(\alpha,\delta)$
- Axial force coefficient (–) $c_Z(\alpha,\delta)$
- Centre of pressure location (m) $Z_{CP}(\alpha,\delta)$ and $Y_{CP}(\alpha,\delta)$

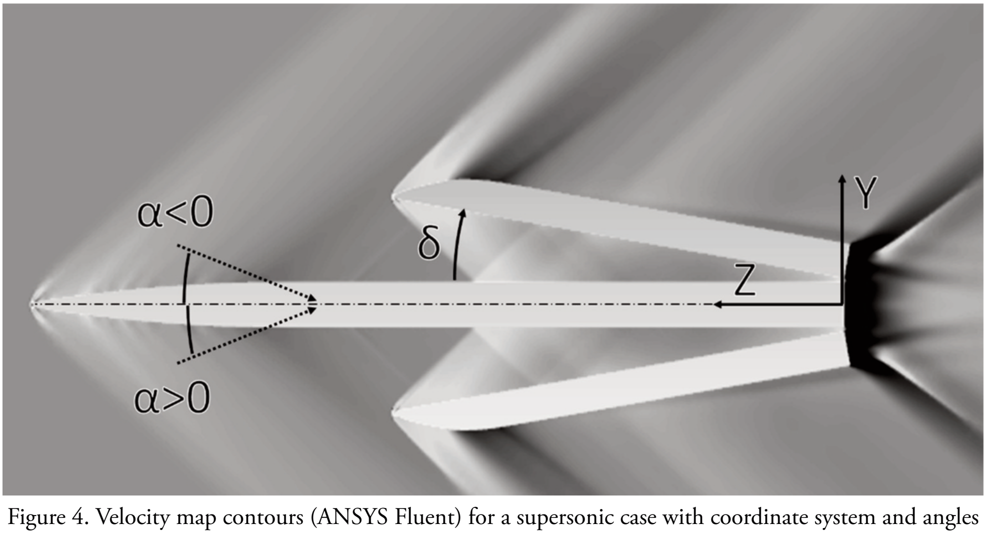

Figure 4. Velocity map contours (ANSYS Fluent) for a supersonic case with coordinate system and angles definitions. 3D symmetry was applied in all cases.

Next, forces acting on the SRB were calculated:

$$F_Y(\delta) = q \cdot c_Y(\delta) \cdot S_{ref.core}$$

$$F_Z(\delta) = q \cdot c_Z(\delta) \cdot S_{ref.core}$$

where q is the dynamic pressure (Pa) acting on the rocket and $S_{ref.core}$ is the reference cross-section area (m^2) based on the main core diameter. The analyses allowed the procurement of valuable data for simulations described in the forthcoming section of the paper. A similar approach was applied in the first version of the ILR-33 AMBER rocket, with smaller boosters [3,13].

It was demonstrated that aerodynamic coefficients and centres of pressure on the SRB are highly dependent on the deflection angle. Due to the nose cone shape and orientation with respect to the core at zero angle of attack, the nose generates negative coefficients $c_Y(\delta)$. That means the SRB is pushed towards the main core. Above the angle of ~4°, aerodynamics start to have a positive impact on the separation process. Achieving this angle during the separation is crucial for its successful execution. Several test cases were conducted combining angles of attack α (from –2° to +2°) with angles of SRB's deflection δ.

As seen in Figure 5, the SRB requires positive deflection angles (higher than nominal zero angle) in order to detach from the rocket. Depending on the rocket's angle of attack α (see definitions in Figure 4), the value varies between 0.75° and 4.25° (worst case).

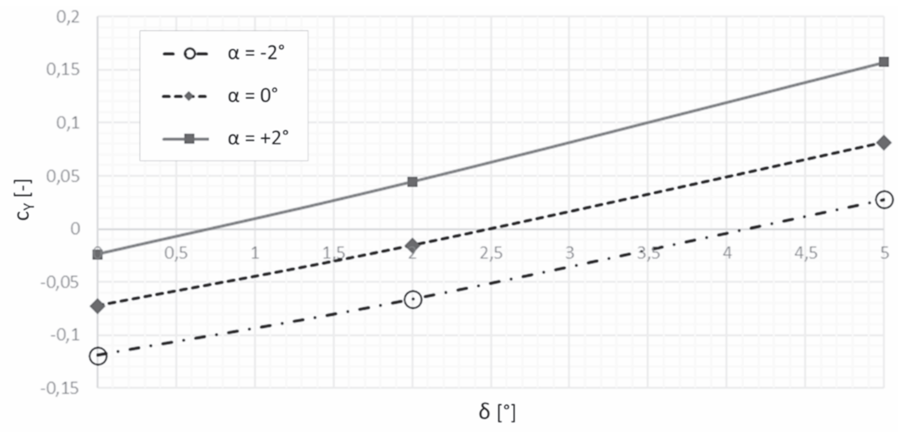

Figure 5. CFD results for SRB normal force behaviour at supersonic velocity (nominal separation conditions). Positive values support the separation, whereas a negative one pushes the SRB towards the core. CFD, computational fluid dynamics; SRB, solid rocket booster.

2.3. Physical modelling of the separation process

A physical model has been created to determine:

- Internal loads acting on each mounting node depending on the external conditions;
- Predicted SRBs trajectories (angular deflection and linear displacement in time) during the separation process, relative to the main core.

External loads from the aerodynamics, thrust and inertia forces were obtained from calculations described in Section 2.2 and from flight ballistics analysis of the rocket executed using the in-house developed code. The mass properties of the SRBs, their moment of inertia and geometrical dimensions were taken from the 3D CAD model and then verified through measurements on the prototypes.

2D 3DOF separation simulations were then conducted, with the use of basic Newton's law equations and geometrical constrains of the system. It is assumed that during separation the loads on both boosters are symmetrical and no other disturbances occur, and accordingly the separation process does not affect the lateral movement of the main core. Three flight cases were analysed: a low-altitude 10 km flight, a medium-altitude 35 km flight and a high-altitude 100 km flight. Optimal repulsing system spring force F_{spr}, release angle δ_{gr} and release delay time Δt_{sep} were found for each of those. The following constrains had to be considered:

- Too low a spring force can cause a lack of sufficient deflection angle and a lack of SRBs separation;
- Too high a spring force can cause local deformation (compression) of the oxidiser tank;
- Too low a release angle can cause a collision between the SRBs and the main core after the separation;
- Too high a release angle can cause excessive (destructive) side forces on the SRB and a trajectory disturbance.

Further design optimisation led to a unification, permitting the use of the same spring and the same release angle for all of the flight cases. Based on the rocket flight analyses of the 10 km and 35 km altitude flights, a separation time delay of several seconds was also introduced to reduce the dynamic pressure during separation and optimise the flight trajectory (results shown in Figure 6).

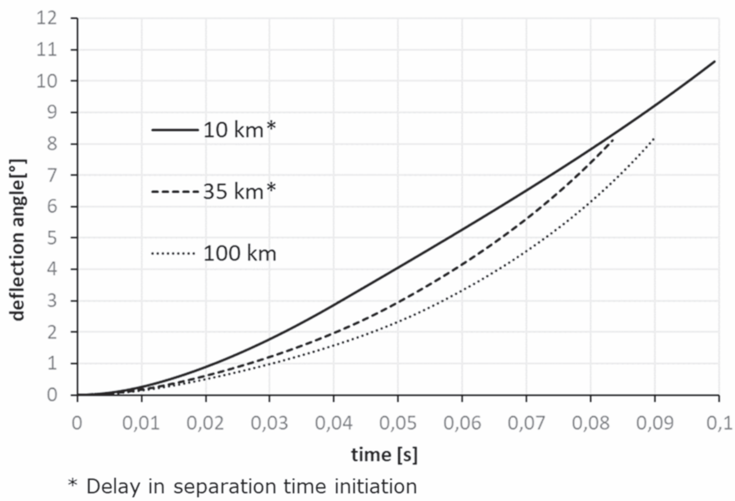

Figure 6. Deflection angle as function of time since separation initiation for chosen flight cases.

3. VERIFICATION, TESTS AND RESULTS

A series of tests were conducted to verify and validate the physical model of the separation.

3.1. Upper node release mechanism functional test

The test was designed to determine the force profile generated by the node in relation to its linear displacement. Although this force is relatively small, compared with the one generated by the repulsing system, it has a significant effect on the separation parameters and has to be considered. A schematic principle of operation is shown in Figure 7. In addition to it, the upper node has a locking mechanism, preventing it from unwanted separation due to external forces.

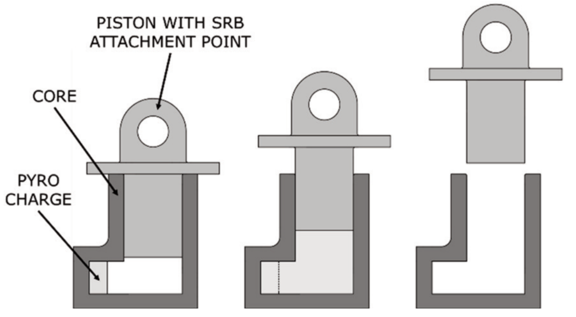

Figure 7. Upper node principle of operation.

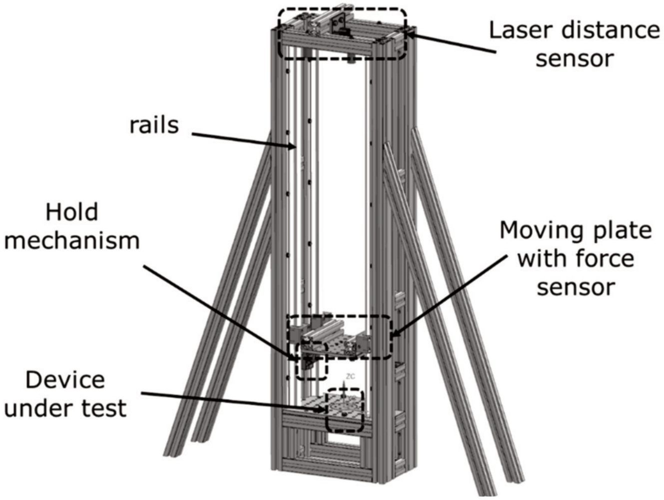

Figure 8. Upper node release mechanism functional test stand.

The test stand (shown in Figure 8) was used to determine crucial parameters of the release mechanism. It consisted of a freely moving plate of a known mass, mounted on rails with linear bearings, a laser distance sensor and a high-speed camera. The following parameters were determined from the gathered data (exemplary results are shown in Figure 9):

- Linear displacement $x(t)$
- Time of operation t_{op}
- Initial force $F_p = F(x_p)$
- End force $F_k = F(x_k)$
- Work $W = \int_{x_p}^{x_k} F(x)\,dx$

During the data analysis, major oscillations of the measured force were observed. With the use of data from the high-speed camera, it was determined that they were caused by vibrations of the plate, onto which the force sensor was mounted. After filtration and correlation of data from the laser sensor and the camera, valuable data were extracted.

A dozen tests of the mechanism in different development configurations have been conducted. All of the tested specimens worked successfully. A high degree of repeatability in terms of forces and time of operation was demonstrated. The gathered data were used to validate and upgrade the separation simulation.

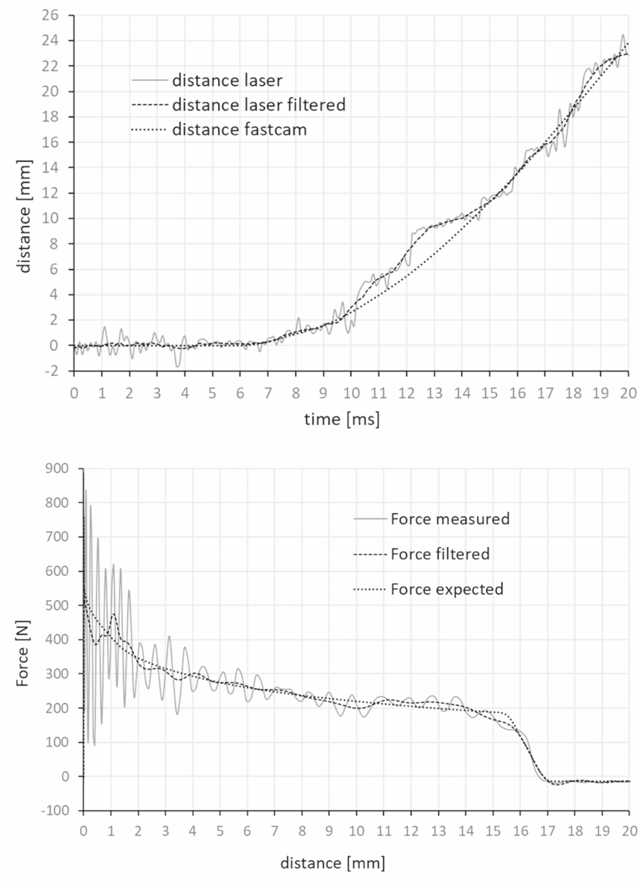

Figure 9. Upper node test results.

3.2. Complete separation system functional test

In conducting the test, the aim was to demonstrate a full separation sequence in various flight cases. Owing to the high variability of the aerodynamic forces depending on the deflection angle, a direct reproduction of flight conditions on the test stand would be complex and very expensive. Accordingly, an alternative approach had been proposed earlier, namely one involving the identification of representative equivalent cases to verify selected separation phases. A test stand (shown in Figure 10) with a dedicated mechanism, consisting of a set of gas springs connected to the SRB, has been used to simulate equivalent forces for each test case. The following parameters were determined from the gathered data:

- Linear displacement $Z(t)$ (sign convention shown in Figure 4)
- Angular displacement $\delta(t)$ (sign convention shown in Figure 4)
- Release angle δ_{gr}
- Time of operation $t_{\delta_{gr}}$

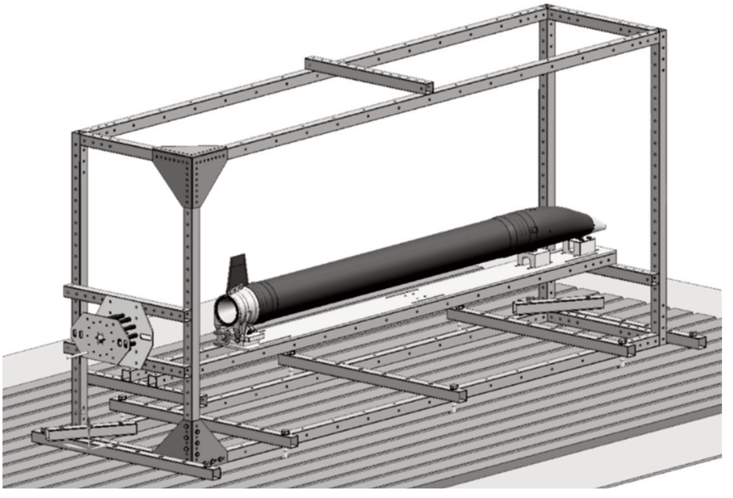

Figure 10. Separation system functional test stand.

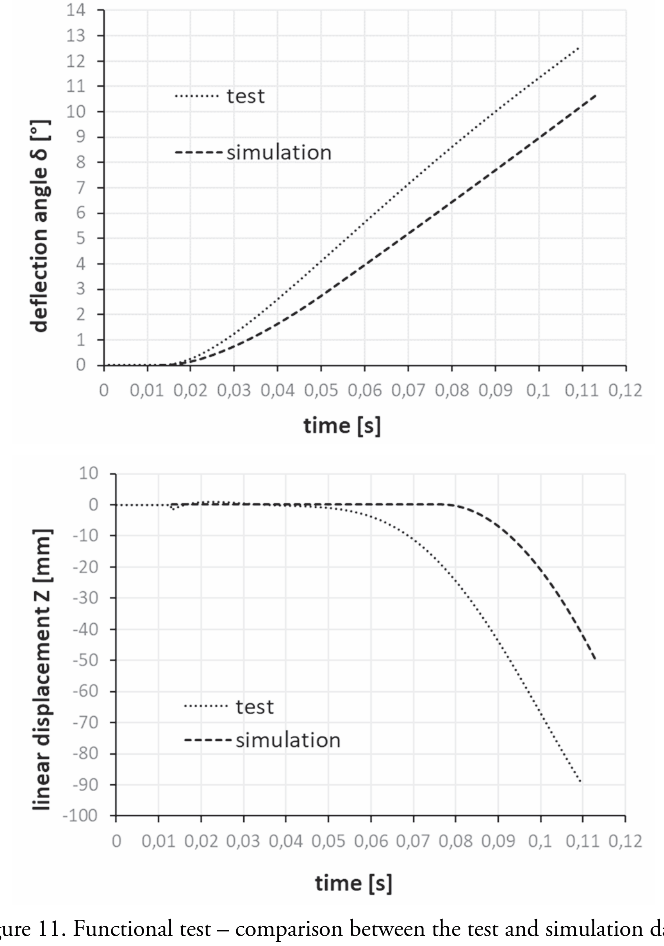

Figure 11. Functional test – comparison between the test and simulation data.

Separation simulations corresponding to these cases were also carried out, using the same physical model and same equations as the flight cases. Next, both experiment and simulations results were correlated, leading to verification and validation of the model (exemplary results are shown in Figure 11, and exemplary frames from the test in Figure 12).

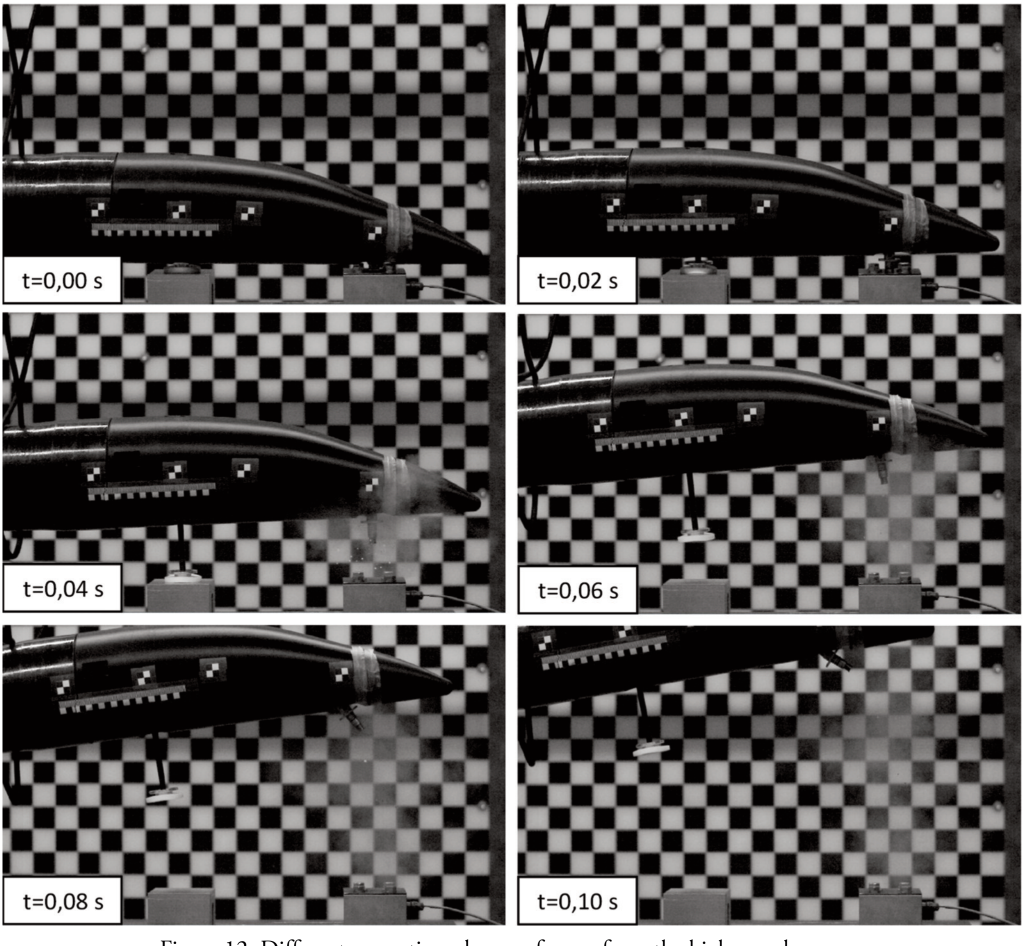

Figure 12. Different separation phases – frames from the high-speed camera.

A fairly accurate correlation between the test and the simulation data was obtained. The angular motion of the SRB begins approximately at the same time and acts with similar dynamics (curve shape). The beginning of the linear motion in the simulation is shifted relative to the test data, but once started, it progresses in a similar way. The discrepancies between both results can be explained by:

- Differences in the moment of inertia in both cases. The moment of inertia of the SRB used in the simulation was obtained from the 3D CAD model and may be inaccurate. An adjustment of the moment of inertia leads to an improvement in the correlation of the deflection angle curve.
- Differences in the release angle (the angle at which the linear displacement begins) in both cases. The measured release angle is smaller than the simulated one, which leads to an earlier commencement of the linear displacement. A reduction of the release angle leads to an improvement in the correlation of the linear displacement curve. These discrepancies can be explained by manufacturing and assembling inaccuracies in the used prototypes.

- Differences in the characteristics of the test stand elements between the model and the real setup.

Despite the demonstrated differences, the results obtained at the test stand are valuable data that prove a proper operation of the separation system in an equivalent environment and can constitute a basis for arriving at a decision regarding qualification of the system for flight tests.

4. DISCUSSION

The results presented above are characterised by a moderate level of accuracy and fidelity. To fully verify the effects of some phenomena, an in-flight test campaign is indispensable. A high degree of system complexity lowers the level of fidelity involved in the dynamic identification of an object. Despite this, the results show that all major effects affecting the separation have been identified and their variations are understood. This qualitative approach allowed qualification of the system for launch.

The authors of this paper are fully aware that the approach shown above is a significantly simplified one in comparison with the analyses performed in the various papers cited within the present study. Contrastingly, this paper also presents a complex approach consisting of a comparison between simulations and test stand results, as well as mathematical model validation, which is rare insofar as separation analyses involving strap-on boosters are concerned. It is caused by a relatively small size of the SRBs and the ILR-33 AMBER 2K rocket as a whole. The authors hope that the presented methodology will be useful for other small rocket designs, where the replacement of advanced computational analysis by an extended test campaign is often profitable in terms of time and schedule and allows a significant increase in the level of reliability and safety during the launch campaign.

5. CONCLUSIONS

The research activities presented in this study were part of a large IoA project, consisting of the design and development of the ILR-33 AMBER 2K rocket. Their aim was to verify the functional requirements of the SRBs separation system and to qualify the chosen design for flight tests.

This task was completed with the use of numerical analysis, including CFD calculations of the separation aerodynamics and 3DOF dynamics simulation. Next, a series of component and system level tests were performed to determine characteristics of key components and to correlate test results with numerical models. Despite the simplifications mentioned in the paper, a good level of correlation has been achieved. The approach presented in the paper has proven to be adequate for the project needs and fully sufficient for the performance of the assigned tasks. In effect, a production of flight-ready components and their acceptance for the launch campaign have been made possible.

However, the following improvements are planned in the next version of the system:

- Minor mechanical design changes, which will facilitate the assembly and the preparation for flight of the subsystems;
- Modifications in the simulation software, which are required to allow for an automated coupling between the separation simulation and the flight dynamics simulation. Currently the simulations are fully independent, which means that separation simulations are performed in quasi-static flight conditions.

The system has been successfully tested during the ILR-33 AMBER 2K low-altitude test flight campaign [14]. However, flight results' correlation with the model is beyond the scope of this paper. The system is currently awaiting verification in high-altitude flights.

Acknowledgments: The research work comprised in this article has been funded by the Łukasiewicz Research Network – Institute of Aviation. The authors are grateful for the support of, and wish to acknowledge, the ILR-33 AMBER project team members, especially Tadeusz Górnicki and Paweł Nowakowski, for their support in the test campaign execution.

REFERENCES

[1] NASA Goddard Space Flight Center, Wallops Flight Facility. "NASA Sounding Rockets User Handbook," 2015.

[2] Cieśliński, D., Noga, T., and Pazik, A. "Polish Civil Rockets' Development Overview." In: *Obronność RP XXI wieku w teorii i praktyce* (2021), Dęblin, Wydawnictwo Lotniczej Akademii Wojskowej: pp. 61–102.

[3] Nowakowski, P., Pakosz, M., Cieśliński, D., Bartkowiak, B., Wolański, P., and Okniński, A. "Development of Small Solid Rocket Boosters for the ILR-33 Sounding Rocket." *Acta Astronautica* Vol. 138 (2017): pp. 374–383. DOI 10.1016/j.actaastro.2017.06.007.

[4] Marciniak, B., Okniński, A., Bartkowiak, B., Pakosz, M., Sobczak, K., Florczuk, W., Kaniewski, D., Matyszewski, J., Nowakowski, P., Cieśliński, D., Rarata, G., Surmacz, P., Kublik, D., Rysak, D., Smętek J., and Wolański, P. "Development of the ILR-33 "Amber" Sounding Rocket for Microgravity Experimentation." *Aerospace Science and Technology* Vol. 73 (2018): pp. 19–31. DOI 10.1016/j.ast.2017.11.034.

[5] Pakosz, M., Noga, T., Kaniewski, D., Okniński, A., and Bartkowiak, B. "24th ESA Symposium on European Rocket and Balloon Programmes and Related Research." In: *ILR-33 AMBER Rocket- Quick, Low Cost and Dedicated Access to Suborbital Flights for Small Experiments*. Essen, 2019.

[6] Pakosz, M., Matysek, K., Nowakowski, P., Noga, T., Majewska, E., and Ptasiński, G. "Design Modifications for Performance Enhancement of a Suborbital Rocket ILR-33 AMBER 2K." In: *71st International Astronautical Congress (IAC) – The Cyber Space Edition*. International Astronautical Federation (IAF), 2020.

[7] Meakin, R.L. "Unsteady Aerodynamic Simulation of Multiple Bodies in Relative Motion: A Prototype Method." American Institute of Aeronautics and Astronautics, NASA Technical Memorandum 102181, 1989.

[8] Lochan, R., Adimurthy, V., and Kumar, K. "Separation Dynamics of Strap-On Boosters." *Journal of Guidance, Control and Dynamics* Vol. 15 No. 1 (1992): pp. 137–143. DOI 10.2514/3.20811.

[9] Lochan, R., Adimurthy, V., and Kumar, K. "Separation Dynamics of Strap-On Boosters in the Atmosphere." *Journal of Guidance, Control and Dynamics* Vol. 20 No. 4 (1997): pp. 633–639. DOI 10.2514/2.4110.

[10] Seongjin, C., Soon-Heum, K., Chongam, K., Oh-Hyun, R., and Jeong-Joo, P. "Numerical Analysis on Separation Dynamics of Strap-On Boosters in the Atmosphere." *KSAS International Journal* Vol. 2 No. 2 (Nov. 2001): pp. 1–17.

[11] AMA Inc., "Aircraft Store Separation and Carriage Loads Analysis: STRLNCH." [Online]. Available at: https://www.ama-inc.com/strlnch. (accessed on 7 September 2022).

[12] Krzysiak, A., Cieśliński, D., Placek, R., and Kekus, P. "Experimental Study of the Boosters Impact on the Rocket Aerodynamic Characteristics." *Aircraft Engineering and Aerospace Technology* Vol. 95 No. 2, (2022): pp. 193–200. DOI 10.1108/AEAT-01-2022-0025.

[13] Ruchała, P., Placek, R., Stryczniewicz, W., Matyszewski, J., Cieśliński, D., and Bartkowiak, B. "Wind Tunnel Tests of Influence of Boosters and Fins on Aerodynamic Characteristics of the Experimental Rocket Platform." *Transactions of the Institute of Aviation* No. 4(249) (2017): pp. 82–102. DOI 10.2478/tar-2017-0030.

[14] Łukasiewicz Research Network – Institute of Aviation. "Pierwsze testy poligonowe rakiety BURSZTYN w wersji 2K i mobilnej wyrzutni rakietowej WR-2." [Online]. Available at: https://ilot.lukasiewicz.gov.pl/pierwsze-testy-poligonowe-rakiety-bursztyn-w-wersji-2k-i-mobilnej-wyrzutni-rakietowej-wr-2/. (accessed on 15 May 2023).